Atmos. Meas. Tech. Discuss., 5, 4447–4472, 2012
www.atmos-meas-tech-discuss.net/5/4447/2012/
doi:10.5194/amtd-5-4447-2012

Atmospheric Measurement Techniques Discussions

Preliminary observation of temperature profiles by radio acoustic sounding system (RASS) with a 1280 MHz lower atmospheric wind profiler at Gadanki, India

T. V. Chandrasekhar Sarma[1], **P. Srinivasulu**[1], **and T. Tsuda**[2]

[1]National Atmospheric Research Laboratory (NARL), Gadanki, 517 112 AP, India
[2]Research Institute for Sustainable Humanosphere (RISH), Kyoto University, Uji 611 0011, Kyoto, Japan

Received: 3 May 2012 – Accepted: 7 June 2012 – Published: 29 June 2012

Correspondence to: T. V. Chandrasekhar Sarma (tvcsarma@narl.gov.in)

Published by Copernicus Publications on behalf of the European Geosciences Union.

Abstract

A UHF wind profiler operating at 1280 MHz has been developed at NARL for atmospheric studies in the planetary boundary layer. In order to explore application of radio acoustic sounding system (RASS) technique to this profiler, a suitable acoustic attachment was designed and preliminary experiments were conducted on 27–30 August 2010. Height profiles of virtual temperature, T_v, in the planetary boundary layer were derived with 1 µs and 0.25 µs pulse transmission, corresponding to a height resolution of 150 m and about 40 m, respectively. Diurnal variation of T_v is clearly recognized, and perturbations of T_v are also seen in association with a precipitation event. Simultaneous profiles obtained from the MST Radar-RASS and an onsite 50 m tower demonstrate the capability to continuously profile the atmospheric temperature from near the ground to upper tropospheric altitudes.

1 Introduction

Ground based remote profiling of atmospheric parameters in the boundary layer is important in the research and operational applications related to industrial pollution dispersion, heat and water vapour flux, air traffic control, satellite launch vehicle sites, nuclear plant installations etc. Measurement of height profiles of wind velocity, temperature and water vapour in the boundary layer have been done using a sodar, a lidar, a wind profiler, and so on. In particular, wind profilers with RASS have been developed for continuously monitoring wind velocity and virtual temperature regardless of weather conditions. May and Wilczak (1993) used a 915 MHz profiler-RASS located near Denver, Colorado to obtain height profiles of wind and virtual temperature in the boundary layer and used them to study the evolution of the nocturnal boundary layer. Using a similar RASS, Angevine et al. (1993) obtained virtual heat flux measurements in the convective boundary layer. They also compared these derivations with the flux measurements from aircraft and found consistency between the measurements as well

AMTD

5, 4447–4472, 2012

Observation of temperature profiles by RASS

T. V. Chandrasekhar Sarma et al.

as theory. A study of the conditions under which RASS derived heat fluxes are reliable was done by Furger et al. (1995). Angevine et al. (1998) compared the wind and temperature measurements from a RASS to those from a 450 m tower. Westwater et al. (1999) compared the temperature profiles from a boundary layer RASS with those from a scanning radiometer. May (1999) studied the structure and thermodynamics of gust fronts over an oceanic site using 920 MHz wind profiler-RASS.

Recently UHF wind profilers working in the upper UHF band (at 1280 MHz) were developed at NARL. Two versions were developed for planetary boundary layer studies. The first one has a transmission peak power of 800 W and an 8 × 8 rectangular patch phased active antenna array of size 1.4 m × 1.4 m (Srinivasulu et al., 2011). This system was operated for some time at NARL in Gadanki (13.46° N, 79.17° E), and it was later moved to a location near Chennai (12.55° N, 80.12° E). A second system with a transmission power of 1.2 kW and a 16 × 16 rectangular patch active antenna array of size 2.8 m × 2.8 m has been in operation at Gadanki (Srinivasulu et al., 2012). Technical details of these radar systems are reported in Srinivasulu et al. (2006). These wind profilers have a range coverage starting from almost near ground (∼100 m) to about 3 km and 5 km for low and high power systems, respectively.

RASS technique was applied to the MST radar of NARL, operated at 53 MHz, and virtual temperature profiles were obtained in the height range of 1.5 km to about 14 km in altitude (Chandrasekhar Sarma et al., 2008, 2011). Height coverage of T_v profiles during some experiments reached altitudes of about 19 km and beyond (Chandrasekhar Sarma, 2011). With the aim of extending the temperature profiling capability at NARL downwards below 1.5 km the RASS technique was applied to the second UHF wind profiler. For this purpose, acoustic attachments were constructed. Preliminary experiments were carried out during 27–30 August 2010 along with MST-Radar RASS at Gadanki. This paper describes the system and presents preliminary results.

2 Experimental set-up

2.1 System description of lower atmospheric wind profiler (LAWP) developed at NARL

The antenna array of LAWP consists of 256 rectangular patch elements at a 0.73λ separation. Consequently, the beamwidth is 5°, first sidelobe level is 16 dB below the main lobe and the grating-lobe free beam steering range is ±20°. Each of the antenna elements is fed by a solid-state TR module generating a peak power of 10 W. The TR module is capable of transmitting a pulsed waveform of duty cycle up to 10 %. The range of pulse widths of transmission is 0.25 µs to 8 µs. Table 1 shows the specifications of the wind profiler system.

Figure 1 shows photographs of the two sets of LAWP. For the smaller LAWP, the 64 antenna elements with a surrounding ground-clutter fence are installed on top of a transportable aluminium cubicle (Srinivasulu et al., 2011). The associated TR modules are attached on the ceiling of the cubicle in order to minimize wiring between the module and antenna elements. Other electronics and a radar control computer are installed in the enclosure below.

The 256 element system was housed in a room in a concrete building of NARL with the antenna kept on the rooftop and TR modules projecting into the room below. Such an arrangement provides an enclosed space that can be environmentally controlled so as to provide ideal temperature, humidity and dust free conditions for efficient performance of radar electronics. Further, the cable transmission losses can be minimised.

2.2 RASS for LAWP

A RASS consists of a wind profiler and a collocated acoustic source (cf. May et al., 1990). The wind profiler is used to measure the Doppler shift due to the acoustic excitation which is proportional to the line of sight apparent sound speed in the direction of the antenna beam. The frequency of the acoustic excitation is chosen so that the wave

AMTD
5, 4447–4472, 2012

number of refractive index perturbations induced in the atmosphere along the radar beam is twice the radar RF transmission wave number. Such a relationship is essential to obtain Bragg scatter from the propagating acoustic wavefronts. The radar measures the wind velocity and the propagation speed of acoustic wavefronts, C_a ($\mathrm{ms^{-1}}$), which is related to ambient temperature T (K),

$$T = \left(\frac{C_a}{k_h}\right)^2. \tag{1}$$

The constant k_h ($\mathrm{J\,K^{-1}\,kg^{-1}}$) in Eq. (1) is given by

$$k_h = \left(\frac{\gamma R}{M}\right)^{\frac{1}{2}} \tag{2}$$

where $\gamma = 1.4$, $R = 8314.472\,\mathrm{J\,K^{-1}\,kmol^{-1}}$ and $M = 28.964\,\mathrm{kg\,kmol^{-1}}$ are ratio of specific heat at constant pressure to specific heat at constant volume, universal gas constant and mean molecular weight of dry air, respectively. For a dry atmosphere k_h works out to be 20.047. RASS determines ambient virtual temperature T_v, which is defined as the temperature that dry air would have if its pressure and density were equal to those of a given sample of moist air. Absolute temperature T and T_v are related as,

$$T_v = (1 + 0.608q)T \tag{3}$$

where q ($\mathrm{kg\,kg^{-1}}$) is the specific humidity which is normally the highest near the surface and decreases exponentially with altitude.

As the radar wavelength of LAWP is 0.23 m corresponding to the 1280 MHz frequency, the acoustic frequency would be 2978.5 Hz for the acoustic speed of 349 $\mathrm{m\,s^{-1}}$ (at 30 °C). Taking a temperature measurement range of 45 °C on the ground to about −10 °C at around 7 km altitude, the acoustic frequency range required would be between 3051 Hz and 2775 Hz. Commercial off-the-shelf components were used for the development of acoustic transmitter due to their easy availability.

AMTD
5, 4447–4472, 2012

The acoustic transmitter consists of a PC-based signal generation, pre-amplifier, power amplifier, compression driver and acoustic horn. Two types of compression drivers were used: high power (JBL 2450H) and lower power (Ahuja AU-60). The JBL2450H driver is an 8 Ohm device with a 150 Wrms continuous output rating for frequencies above 1 kHz. The AU-60 is a 16 Ohm device with a 60 Wrms and 90 W peak rating and 132 dB SPL at 1 m. The acoustic horn is also made by Ahuja Radios (Ahuja WFB) and is suitable for direct use with AU-60; these products are meant for public address systems. To allow mounting of JBL2450H, the horn was modified to accommodate the larger throat diameter of this compression driver.

Figure 2 shows the horn arrangement. Each of the horns was mounted in a mild steel frame so that it would point upwards and could be deployed in the field. It is an exponential horn folded twice in a reflex design as shown in Fig. 2a. The horn is made of aluminium with a mouth diameter of 18 inch (45.7 cm) and has lower cutoff frequency of 190 Hz. It can accommodate a compression driver of outer throat diameter 3.5 cm. This horn was chosen due to its broad frequency response, easy local availability, low cost and suitability for outdoor use. The AU-60 is a suitable driver for direct use with the WFB. Further it is also made of aluminium and is suitable for continuous outdoor use as the WFB. For use with JBL2450H the horn was modified as shown in Fig. 2b. In this arrangement the driver was mounted at the second fold of the horn where the diameter of the horn is greater than that of the throat diameter of the driver using a poly vinyl chloride (PVC) pipe and PVC coupling. The portion of the reflex horn below that diameter was removed. In both of the configurations, three holes were drilled at the bottom of the horn to allow drainage of rainwater.

The signal generation is based on a notebook personal computer for flexibility in waveform design and compact footprint. A MATLAB programme was generated which would compute the voltages for a chirped waveform between the low and high frequencies of the acoustic excitation required to satisfy Bragg scatter condition between the expected temperature extremes. The file was stored in .wav format and was played using commonly available media player programmes like the Windows Media Player,

AMTD
5, 4447–4472, 2012

Real Player or the VLC Media Player. The notebook PC has a stereo headphone output from which the voltages corresponding to the digital data being played out on the PC is available. This output is connected to the input of a Sonifex RB-UL4 unbalanced to balanced converter preamplifier. The pre-amplifier converts the two single ended inputs to two differential outputs along with ground in the XLR connector format, suitable for driving the voltages over long distances up to the power amplifier and also providing common mode noise rejection. The outputs of the preamplifier form inputs to Crown CL2 power amplifier. The compression drivers are driven from the outputs of the power amplifier. The electronics are kept inside the room. The acoustic transmission system described in the previous section was tested at a 3 kHz tone for checking the power output. With the JBL2450H the maximum SPL that could be achieved was 128 dB at the mouth of the horn, and using AU-60 it was 118 dB.

The SPL output using AU-60 at 1 m above the horn mouth with respect to the input electrical power is plotted in Fig. 3. The radiation pattern of the horn with Ahuja AU-60 was measured as shown in Fig. 4. The 3 dB beamwidth is about 40° and emitted level towards the horizon is about 20 dB below that in the vertical direction. A relatively narrow beam is useful in directing major portion of the energy towards vertical direction and is preferable as the atmospheric attenuation at around 3 kHz is severe. High level of atmospheric attenuation limits the range coverage of the RASS. Use of high power transmitter would be intuitively more suitable for better range coverage performance. But preliminary results showed that the maximum range coverage was about similar with either of these transmitters. Though it needs further investigation, limitations due to the background wind field seem to dominate the range coverage performance of RASS. Distortion of the acoustic wavefronts due to turbulence is an additional contributing factor. It has been analytically shown that the range coverage performance of a RASS depends on the background wind conditions and turbulence (Clifford and Wang, 1977; Lataitis, 1992). Masuda (1988) has formulated an analytical framework based on acoustic ray-tracing to find out the optimum beam direction for maximum range coverage.

AMTD
5, 4447–4472, 2012

3 Coordinated RASS observations with LAWP and MST radars

3.1 Observation scheme of LAWP

Using the LAWP-RASS, a preliminary experiment was conducted. The experiment was started with the high power exciter at around 09:30 LT on 27 August 2010. However, the high power exciters failed probably due to thermal heating as they are mounted on top and the rain protection cover (not shown in Fig. 2) did not allow heat dissipation. Then the system was switched to use the AU-60 exciter and the experiment was restarted at around 17:20 LT on 27 August 2010. The experiment continued until about 03:00 LT on 28 August 2010 and stopped due to failure of power amplifier. The power amplifier was replaced and the experiment was restarted around 13:00 LT on 28 August 2010 and was continued up to 13:00 LT on 30 August 2010.

The specifications of the experiment with LAWP-RASS are shown in Table 2. The acoustic source was swept between 3003 Hz and 2929 Hz corresponding to temperatures of 35 °C and 20 °C, respectively. In this experiment four modes of operation were carried out viz., RASS mode 1, correction wind mode, background wind mode and RASS mode 2. In the present wind profiler system, there is provision to run only up to a maximum of four experimental specifications sequentially. The RASS mode 1 is that for measuring the line of sight speed of acoustic wavefronts. Correction wind mode 1 is intended to record the line of sight wind speed and use it to correct the apparent speed recorded in RASS mode 1. Background wind mode 1 is intended for recording the three-dimensional wind field. In these three modes, the lowest range from which recording can start is 300 m and the range resolution is 150 m corresponding to 1 µs transmission.

To extend the lowest height of observation below 300 m, a fine range resolution mode viz., RASS mode 2 was tested. In this mode the pulse width of transmission is 0.25 µs and the corresponding range resolution is 37.5 m. Due to the current limitation of the number of specifications being run in a sequence, correction wind mode of the second rass mode could not be conducted. It would be possible to use the three-beam

AMTD
5, 4447–4472, 2012

observation from a colocated SODAR (Anandan et al., 2008) but as the data was not reliable above 150 m it could not be used.

Figure 5a–d shows typical spectra in respectively the RASS mode 1, correction wind mode 1, RASS mode 2 and background wind mode 1. Figure 5a shows the range coverage of the 1 µs operation with LAWP-RASS. The RASS echo was obtained up to 1.2 km. The maximum height coverage with both high power system and lower power system is similar; better SNR resulted when using the higher power system. This preliminary result indicates that height coverage is limited by the background wind conditions at surface and aloft. Figure 5d shows the coverage with 0.25 µs pulse operation. The lowest range from which signal is available is around 200 m and the maximum height reached is about 800 m. The lowest heights below 200 m do not have any signal. This could be due to the separation between the antenna array and the acoustic source. Due to the nature of the LAWP antenna, acoustic source cannot be kept at the center of the antenna array. However, if the acoustic sources can be accommodated into the antenna by appropriate design it would be useful to obtain echoes from the lowest height possible. The lowest height in a monostatic radar is limited by the T/R switch recovery time and the antenna size (which determines the distance to the far field).

The Doppler spectra were subjected to moments computation by fitting a Gaussian curve to the individual spectra in each range bin. The mean Doppler of RASS echo so computed needs correction by subtracting the Doppler shift of the turbulence echo in the same beam direction to obtain the Doppler shift due to the true sound speed. However, as the 1280 MHz frequency is highly sensitive to precipitation leading to stronger echoes, the turbulence Doppler spectrum in the lower ranges, at which RASS echo was obtained, is contaminated. As a result, the retrieved Doppler is in error. Therefore correcting the RASS apparent Doppler shift in this method was not feasible. A solution was found in the way the experiment was done. It is noted that RASS observation was done along five beams, viz., one zenith and four 5° off zenith in E, W, N and S directions. As the atmospheric motions are homogeneous over the cone of volume covered by the wind profiler beams, when vertical wind is neglected, the line of sight Doppler shifts due to turbulence along coplanar beams symmetrical about the zenith would be same in absolute values only with signs being opposite. Using this method the Doppler shift due to the acoustic speed was computed by averaging the observed Doppler shifts in symmetrical beams, viz., E and W and N and S wherever RASS echo was present. Such a facility was not available in the 0.25 µs observation as the echo was not present in the recordings of all the symmetric beam directions.

3.2 MST radar-RASS observations

During this experiment MST radar RASS was also operated along with the wind profiler-RASS on 27–30 August 2010. Experimental specifications used for MST radar-RASS are shown in Table 3. The corresponding acoustic sources generated swept frequency waveform in the range 125 Hz to 94 Hz corresponding to temperatures of −90 °C and 40 °C, respectively. An example of typical spectra from MST radar-RASS can be found in Chandrasekhar Sarma et al. (2011).

4 Results and discussion

4.1 Background meteorological conditions

During this experiment, the sky was mostly cloudy and visual observations during daylight hours showed many specks of cloud moving with the wind over the wind profiler site at a very low altitude of about 200 m. Further, there were occasional rain showers. Pictures from an onsite all sky imager showed an overcast sky with occasional clearings on the morning of 27 and 28 August.

An onsite 50 m tower recorded the temperature, humidity, wind speed and direction at six levels above ground at 2, 4, 8, 16, 32 and 50 m. Rainfall and surface pressure were also recorded. Figure 6a shows the plots of virtual temperature at all the levels.

AMTD
5, 4447–4472, 2012

Figure 6b shows the rain rate. Simultaneous TRMM-TOVAS satellite observations also revealed presence of scattered precipitation over the region of peninsular India.

4.2 Continuous temperature profile between 0.5 and 10 km altitude on 27 August 2010

Figure 7 shows a colour coded plot of T_v profiles obtained during 27–30 August 2010 using MST radar for about 72 h. The height coverage of the T_v retrieval reached up to 12 km in altitude on the first day. However, later on due to changes in the wind field, failure of some acoustic exciters and rainfall, acoustic echo was missing. When the acoustic echo was present during rainfall, the wind Doppler spectrum was contaminated and T_v retrieval was unstable. In order to enhance the visual perception of diurnal temperature variation at lower tropospheric altitudes, T_v profiles are shown only up to 5 km in Fig. 7.

Figure 8a shows the colour coded plot of T_v retrievals from 1 µs observations of LAWP-RASS. It shows that most of the time the T_v retrieval was only up to 750 m altitude. This is because, even though acoustic echo was available up to about 1.0 km, due to absence of echo in the symmetric beam directions, retrieval could not be done. The T_v retrievals from 0.25 µs observation are shown Fig. 8b as a colour coded plot. The height coverage of the 0.25 µs reached up to about 800 m. With the addition of LAWP-RASS, the temperature profiling capability at NARL has been extended from ground to above the tropopause. Figure 9a shows a stackplot of the T_v from 1 µs observations shown in Fig. 8a. Similarly, Fig. 9b shows a stackplot of T_v from the 0.25 µs observation shown in Fig. 8b.

4.3 Diurnal variations of the temperature

From Fig. 9a and b, we see that the effect of diurnal variation of ground temperature as illustrated by data from 50 m tower (shown in Fig. 6a) is evident in the diurnal variation of T_v at heights up to 900 m. Such a phenomenon can also be seen at the lowest height

AMTD
5, 4447–4472, 2012

in the MST Radar RASS observations shown in Fig. 7. The periodogram analysis of the T_v profiles shows that the maxima in the temperature occur around 14:00 LT at lower heights whereas they are progressively delayed as altitude increases. The amplitudes of the diurnal temperature variation due to surface heating also decrease with altitude. The maximum virtual temperatures at heights of 2 m, 8 m and 50 m occur around 14:00 LT. These values on 28th August are respectively 37 °C, 36.3 °C and 35.3 °C, respectively and on 29 August they are 35 °C, 34.6 °C and 33.6 °C, respectively. From the virtual temperatures derived using 0.25 µs pulse transmission data of 29 August, maxima at heights 262.5 m, 300 m, 337.5 m, 375 m, 412.5 m, 450 m, 487.5 m, 525 m, 562.5 m, 600 m occur respectively at 19:36 LT, 19:17 LT, 19:27 LT, 19:23 LT, 19:41 LT, 19:51 LT, 20:27 LT, 20:27 LT, 20:42 LT, 20:30 LT. The temperature maxima are respectively 31.09 °C, 31.28 °C, 31.16 °C, 31.15 °C, 31.09 °C, 30.98 °C, 30.54 °C, 30.53 °C 30.41 °C, 30.49 °C. This phenomenon delineates the boundary layer from the free troposphere. Using the T_v data the height of the boundary layer could be clearly delineated. Usually the boundary layer height extends up to about 3.5 km at Gadanki. However, as this preliminary experiment was conducted on an overcast day, signatures of boundary layer height could be discerned only up to the lowest range bins of MST radar-RASS observations viz., up to about 2.5 km.

5 Summary

We present the application of RASS technique to a UHF (1280 MHz) wind profiler. The wind profiler-RASS was operated in two modes. One with standard resolution of 150 m and another with a finer resolution of 37.5 m. The former mode covered the range from 450 m to 1.2 km. The latter mode covered the lower heights starting at about 200 m up to ~800 m. Due to the problem of contamination of turbulence Doppler spectra by hydrometeors, the RASS acoustic Doppler frequency obtained in symmetrical beams was used to correct for the effect of background wind. The error introduced in temperature measurement is limited to the effect of vertical wind speed.

Data obtained from the operation of the LAWP-RASS along with data from 50 m tower and MST-Radar RASS extended the height coverage of temperature profiling from near ground up to upper tropospheric heights and potentially beyond the tropopause.

Acknowledgements. National Atmospheric Research Laboratory is a grants-in-aid institution of the Department of Space, Government of India. The first author acknowledges the support from Atmospheric Science Programme office of Department of Space by way of funding for the RASS project. He also acknowledges the financial support by Japan Society for Promotion of Science to cover research trips to Japan by way of Ronpaku fellowship during the financial years 2006–2010.

References

Anandan, V. K., Kumar, M. S., and Rao, I. S.: First results of experimental tests of the newly developed NARL phased-array Doppler Sodar, J. Atmos. Ocean. Tech., 25, 1778–1784, 2008.

Angevine, W. M., Avery, S. K., and Kok, G. L.: Virtual heat flux measurements from a boundary-layer profiler-RASS compared to aircraft measurements, J. Appl. Meteorol., 32, 1901–1907, 1993.

Angevine, W. M., Bakwin, P. S., and Davis, K. J.: Wind profiler and RASS measurements compared with measurements from a 450-m-tall tower, J. Atmos. Ocean. Tech., 15, 818–825, 1998.

Chandrasekhar Sarma, T. V.: Design and Development of Radio Acoustic Sounding System with the Indian MST Radar, PhD thesis, Kyoto University, Kyoto, Japan, 2011.

Chandrasekhar Sarma, T. V., Narayana Rao, D., Furumoto, J., and Tsuda, T.: Development of radio acoustic sounding system (RASS) with Gadanki MST radar – first results, Ann. Geophys., 26, 2531–2542, doi:10.5194/angeo-26-2531-2008, 2008.

Chandrasekhar Sarma, T. V., Kodama, Y.-M., and Tsuda, T.: Characteristics of atmospheric waves observed in the upper troposphere observed with the Gadanki MST radar-RASS, J. Atmos. Sol.-Terr. Phys., 73, 1020–1030, 2011.

Clifford, S. and Wang, T.: The range limitation on radar-acoustic sounding systems (RASS) due to atmospheric refractive turbulence, IEEE T. Antenn. Propag., 25, 319–326, 1977.

AMTD
5, 4447–4472, 2012

Observation of temperature profiles by RASS

T. V. Chandrasekhar Sarma et al.

Furger, M., Whiteman, C. D., and Wilczak, J. M.: Uncertainty of boundary layer heat budgets computed from wind profiler-RASS networks, Mon. Weather Rev., 123, 790–799, 1995.

Lataitis, R. J.: Signal power for radio acoustic sounding of temperature: the effects of horizontal winds, turbulence, and vertical temperature gradients, Radio Sci., 27, 369–385, 1992.

Masuda, Y.: Influence of wind and temperature on the height limit of a radio acoustic sounding system, Radio Sci., 23, 647–654, 1988.

May, P. T.: Thermodynamic and vertical velocity structure of two gust fronts observed with a wind profiler/RASS during MCTEX, Mon. Weather Rev., 127, 1796–1807, 1999.

May, P. T. and Wilczak, J. M.: Diurnal and seasonal variations of boundary-layer structure observed with a radar wind profiler and RASS, Mon. Weather Rev., 121, 673–682, 1993.

May, P. T., Strauch, R. G., Moran, K. P., and Ecklund, W. L.: Temperature sounding by RASS with wind profiler radars: a preliminary study, IEEE T. Geosci. Remote Sens., 28, 19–28, 1990.

Srinivasulu, P., Padhy, M. R., Yasodha, P., and Narayana Rao, T.: Development of UHF Wind Profiling Radar for Lower Atmospheric Research Applications: Preliminary Design Report, National Atmospheric Research Laboratory, Gadanki, India, 2006.

Srinivasulu, P., Yasodha, P., Jayaraman, A., Reddy, S. N., and Satyanarayana, S.: Simplified active array L-band radar for atmospheric wind profiling: initial results, J. Atmos. Ocean Tech., 28, 1436–1447, 2011.

Srinivasulu, P., Yasodha, P., Reddy, S. N., Kamaraj, P., Narayana Rao, T., Satyanarayana, S., and Jayaraman, A.: 1280 MHz active array radar wind profiler for lower atmosphere: system description and data validation, J. Atmos. Ocean. Tech., doi:10.1175/JTECH-D-12-00030.1, in press, 2012.

Westwater, E. R., Han, Y., Irisov, V. G., Leuskiy, V., Kadygrov, E. N., and Viazankin, S. A.: Remote sensing of boundary layer temperature profiles by a scanning 5-mm microwave radiometer and RASS: comparison experiments, J. Atmos. Ocean. Tech., 16, 805–818, 1999.

AMTD

5, 4447–4472, 2012

Table 1. Specifications of the 16 × 16 lower atmospheric wind profiler at Gadanki.

Parameter	Specification
Frequency	1280 MHz
Antenna type	256 element microstrip patch array arranged in a 16 × 16 matrix of size 2.8 m × 2.8 m
Antenna beam width	5°
Beam former	Passive (Modified Butler Matrix)
Beams directions	Five [(11°, 15°), (101°, 15°), (0°, 0°), (191°, 15°) and (281°, 15°)]
Tx/Rx type	Solid state transceivers
Peak power	1.2 kW
Duty ratio	Up to 10 %
Pulse width	0.25 µs–8.0 µs
NCI	4–1000
NFFT	32–1024
Range bins	1–256
Receiver	Super heterodyne
Dynamic range	70 dB
Minimum height	112.5 m

AMTD
5, 4447–4472, 2012

Table 2. Experimental parameters of LAWP-RASS operation.

Parameter	RASS mode 1	Correction wind mode 1	Background wind mode 1	RASS mode 2
Pulse Width (μs)	1.0	1.0	1.0	0.25
Range resolution (m)	150	150	150	37.5
Inter Pulse Period (μs)	55	55	55	25
Beam sequence	E5°, W5°, Z, N5°, S5°	E5°, W5°, Z, N5°, S5°	E15°, W15°, Z, N15°, S15°	E5°, W5°, Z, N5°,S5°
No. of coherent integrations	32	256	32	32
No. of FFT points	512	256	512	1024
No. of online incoherent integrations	20	10	20	20
Start of observation range window	300 m	300 m	300 m	112.5 m
No. of range bins	40	40	40	55
Second LO offset frequency	−3000 Hz	0 Hz	0 Hz	−3000 Hz
Time duration	∼2.0 min	∼3.0 min	∼1.0 min	∼1.5 min
Acoustic frequency sweep range	3003 Hz to 2929 Hz			
Acoustic excitation duty	5 s ON, 1 s OFF			

AMTD
5, 4447–4472, 2012

Table 3. Experimental specifications of MST-RASS operation.

Parameter	RASS mode	Correction wind mode	Background wind mode
Pulse Width (µs)	1	1	1
Range resolution (m)	150	150	150
Inter Pulse Period (µs)	250	250	250
Beam sequence	Chosen based on ray tracing result	Same as in RASS mode	E20°, W20°, Zy*, Zx*, N20°, S20°
No. of coherent integrations	96	128	128
No. of FFT points	256	256	512
No. of online incoherent integrations	8	8	2
Start of observation range window	1.5 km	1.5 km	1.5 km
No. of range bins	160	160	160
Second LO offset frequency	−110 Hz	0 Hz	0 Hz
Time duration	∼3.5 min	∼4.5 min	∼4 min
Acoustic frequency sweep range		125 Hz to 94 Hz	
Acoustic excitation duty		4 s ON, 2 s OFF	

* Zx and Zy – Zenith beams formed using N–S and E–W dipoles, respectively.

AMTD
5, 4447–4472, 2012

(a) (b)

Fig. 1. (a) The 64 element wind profiler with enclosure and antenna array on the top. **(b)** The rooftop antenna with clutter fence of the 256 element wind profiler along with acoustic exciters.

AMTD
5, 4447–4472, 2012

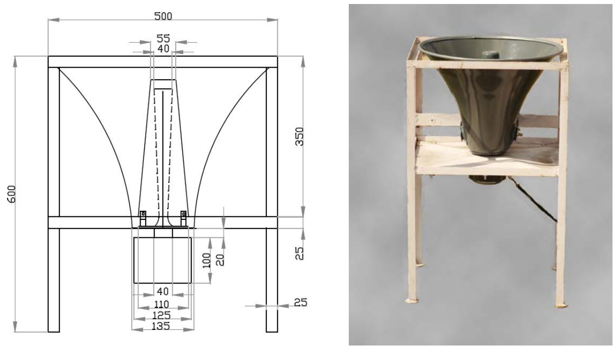

(a)

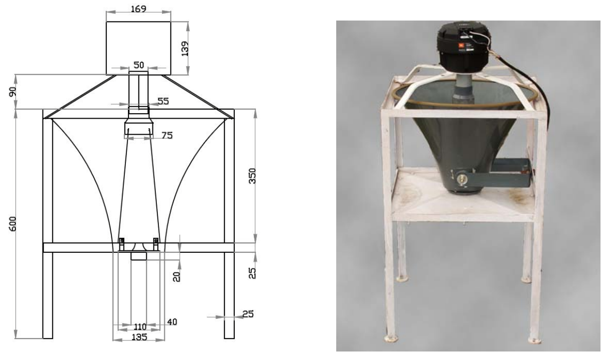

(b)

Fig. 2. (a) Horn cross section with AU-60 mounted at the bottom and its photographs. **(b)** Horn cross section with JBL2450H mounted on the top and its photograph. All dimensions are in mm.

AMTD
5, 4447–4472, 2012

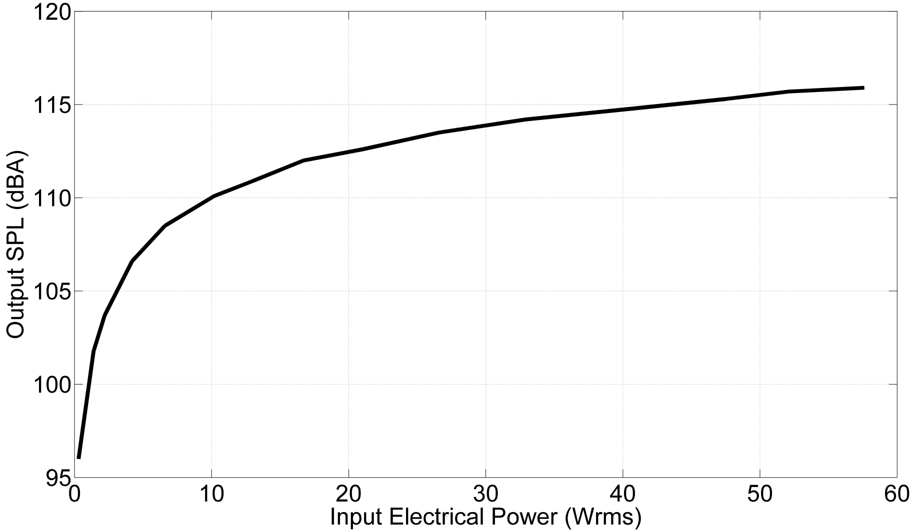

Fig. 3. Input electrical power versus sound pressure level output of the horn using AU-60 driver. Measurements were made 1 m above the mouth of the horn.

AMTD
5, 4447–4472, 2012

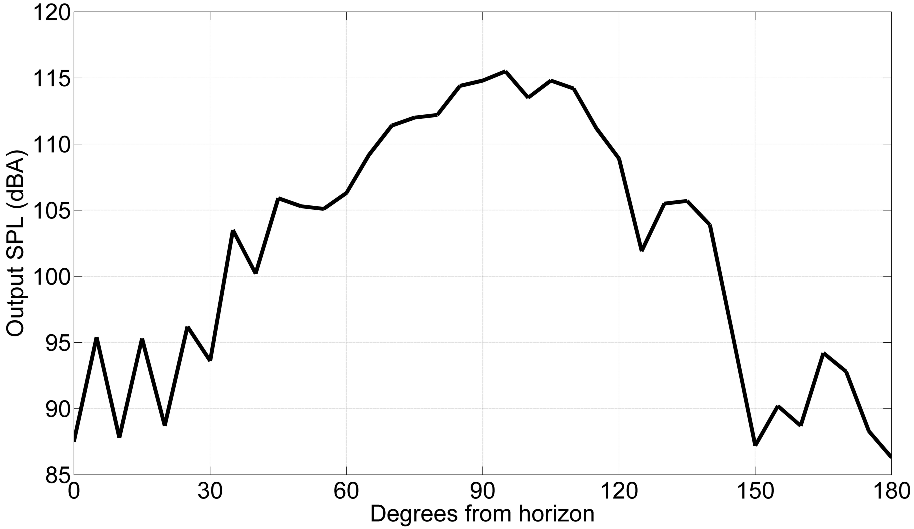

Fig. 4. Radiation pattern of the Ahuja WFB horn with AU-60 compression driver.

AMTD
5, 4447–4472, 2012

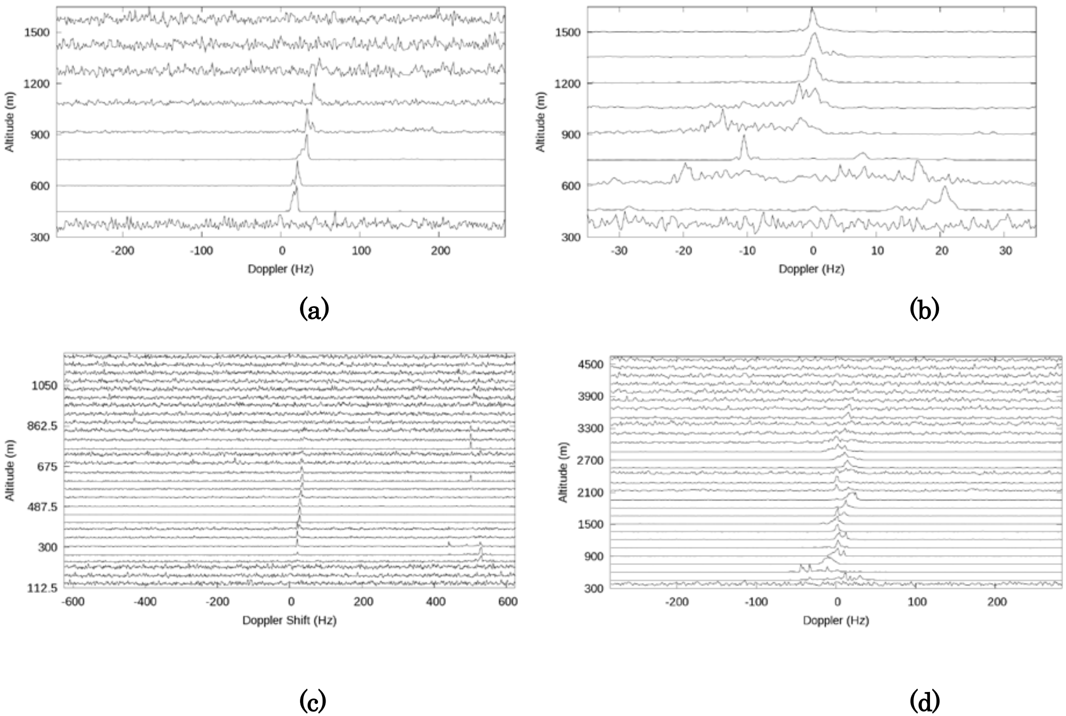

Fig. 5. Typical Doppler spectra obtained from WP-RASS. **(a)** acoustic echo with 1 µs transmission. **(b)** 5° Turbulence echo with 1 µs transmission; **(c)** acoustic echo with 0.25 µs transmission; **(d)** 15° turbulence echo with 1 µs transmission.

AMTD

5, 4447–4472, 2012

Observation of temperature profiles by RASS

T. V. Chandrasekhar Sarma et al.

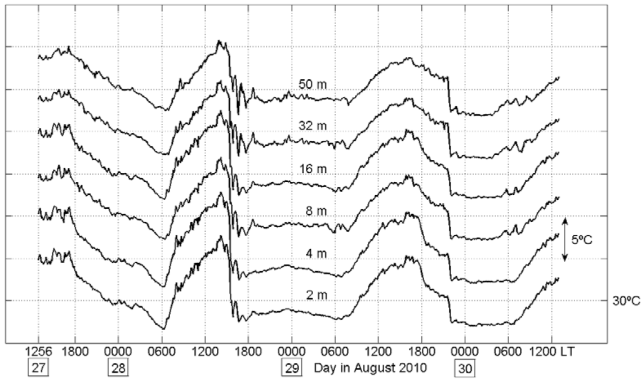

(a)

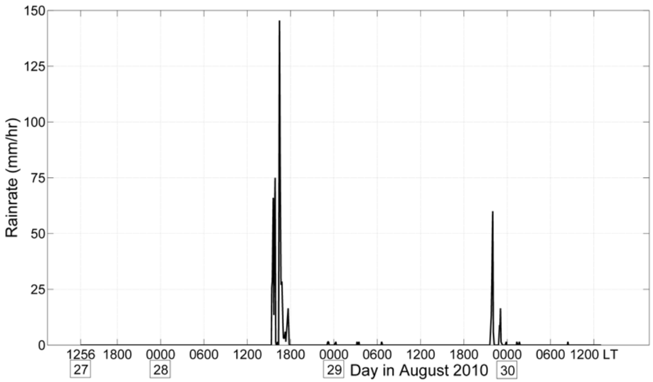

(b)

Fig. 6. (a) Virtual temperature at the six levels of the 50 m tower; **(b)** rainrate measured near the 50 m tower.

AMTD
5, 4447–4472, 2012

Observation of temperature profiles by RASS

T. V. Chandrasekhar Sarma et al.

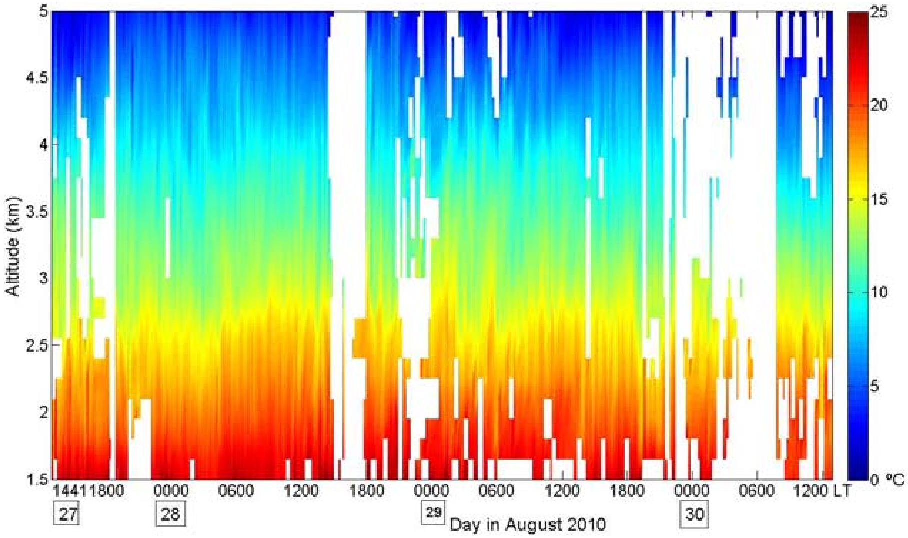

Fig. 7. The T_v observations using MST radar-RASS starting at 12:54 LT on 27 August 2010 and going on upto 13:30 LT on 30 August 2010.

AMTD
5, 4447–4472, 2012

Observation of temperature profiles by RASS

T. V. Chandrasekhar Sarma et al.

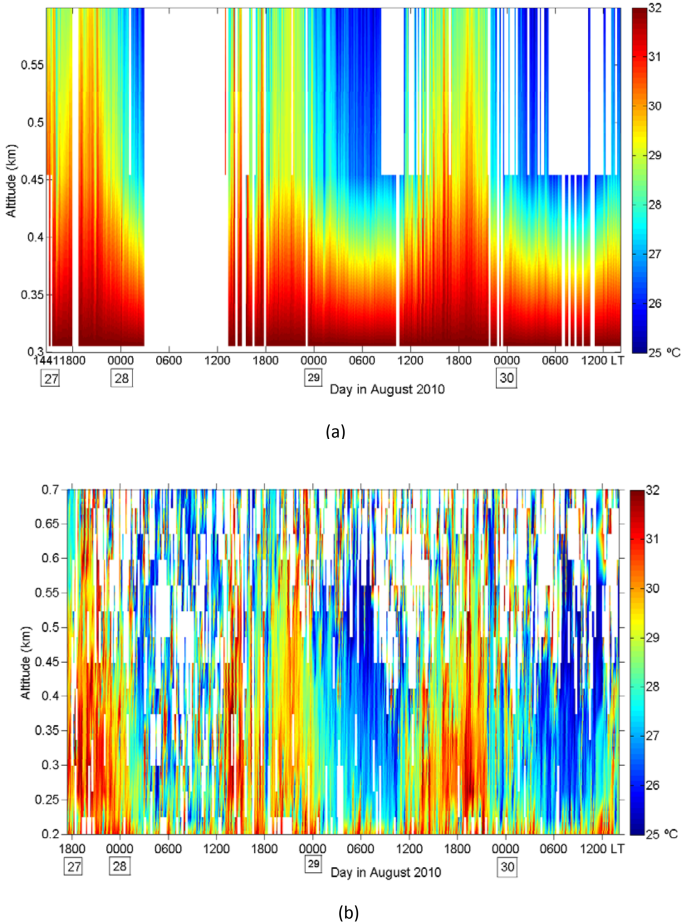

Fig. 8. (a) Colour coded plot of T_v observations using 1 µs operation of WP-RASS; **(b)** colour coded plot of T_v observations using 0.25 µs operation of WP-RASS.

AMTD
5, 4447–4472, 2012

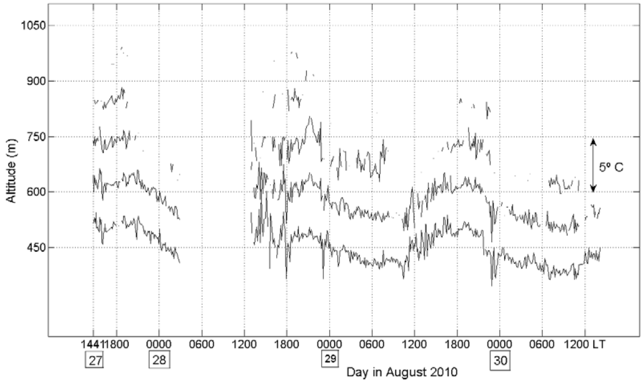

(a)

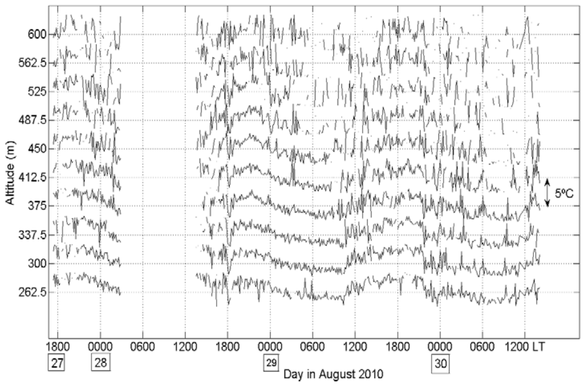

(b)

Fig. 9. (a) Line plot of the time series of virtual temperature using 1 µs observation; **(b)** line plot of the time series of virtual temperature using 0.25 µs observation.